The Astrophysical Journal, 630:1160–1167, 2005 September 10

SEQUENTIAL CHROMOSPHERIC BRIGHTENINGS BENEATH A TRANSEQUATORIAL HALO CORONAL MASS EJECTION

K. S. Balasubramaniam, A. A. Pevtsov, and D. F. Neidig[1]
National Solar Observatory,[2] Sunspot, NM 88349; bala@nso.edu, apevtsov@nso.edu

E. W. Cliver
AFRL Space Vehicles Directorate, Space Weather Center of Excellence, Hanscom AFB, MA 01731

B. J. Thompson
NASA Goddard Space Flight Center, Greenbelt, MD 20771

C. A. Young
L3 Communication, NASA Goddard Space Flight Center, Greenbelt, MD 20771

S. F. Martin
Helio Research, 5212 Maryland Avenue, La Crescenta, CA 91214

and

A. Kiplinger
Center for Integrated Plasma Studies, University of Colorado, Boulder, CO 80309; and NOAA Space Environment Center, 325 Broadway, Boulder, CO 80303
Received 2005 February 8; accepted 2005 May 18

ABSTRACT

Analyses of multiwavelength data sets for a solar eruption at ~21:30 UT on 2002 December 19 show evidence for the disappearance of a large-scale, transequatorial coronal loop (TL). In addition, coronal manifestations of the eruption (based on *SOHO* EIT and LASCO images) include large-scale coronal dimming, flares in each associated active region in the northern and southern hemispheres, and a halo CME. We present detailed observations of the chromospheric aspects of this event based on Hα images obtained with the ISOON telescope. The ISOON images reveal distant flare precursor brightenings, sympathetic flares, and, of most interest herein, four nearly cospatial propagating chromospheric brightenings. The speeds of the propagating disturbances causing these brightenings are 600–800 km s^{-1}. The inferred propagating disturbances have some of the characteristics of Hα and EIT flare waves (e.g., speed, apparent emanation from the flare site, subsequent filament activation). However, they differ from typical Hα chromospheric flare waves (also known as Moreton waves) because of their absence in off-band Hα images, small angular arc of propagation ($<30^\circ$), and their multiplicity. Three of the four propagating disturbances consist of a series of sequential chromospheric brightenings of network points that suddenly brighten in the area beneath the TL that disappeared earlier. *SOHO* MDI magnetograms show that the successively brightened points that define the inferred propagating disturbances were exclusively of one polarity, corresponding to the dominant polarity of the affected region. We speculate that the sequential chromospheric brightenings represent footpoints of field lines that extend into the corona, where they are energized in sequence by magnetic reconnection as coronal fields tear away from the chromosphere during the eruption of the transequatorial CME. We report briefly on three other events with similar narrow propagating disturbances that were confined to a single hemisphere.

Subject headings: stars: activity — stars: magnetic fields — Sun: activity — Sun: coronal mass ejections (CMEs) — Sun: flares — Sun: magnetic fields — Sun: photosphere — sunspots

1. INTRODUCTION

Chromospheric flare waves and coronal (*Solar and Heliospheric Observatory* [*SOHO*] Extreme-Ultraviolet Imaging Telescope [EIT]) flare waves are large-scale disturbances that propagate away from solar flares and/or the launch sites of coronal mass ejections (CMEs). The classic chromospheric flare wave, also known as a Moreton wave (Moreton 1960; Athay & Moreton 1961; Dodson & Hedeman 1964; Dodson & Hedeman 1968; Smith & Harvey 1971), appears in images in the wings of Hα as both bright and dark parallel fronts propagating in an arc, away from the site of solar flare. The bright/dark front (or dark/bright in the opposite wing of Hα) is due to the successive depression and relaxation of chromospheric structures caused by the pressure of an overlying coronal wave assumed to propagate at high velocity through the corona from the site of a solar flare. The downward and upward oscillation of the chromosphere damps out after only one to two oscillations. Similar sudden vertical oscillations in filaments (Dodson & Hedeman 1964; Ramsey & Smith 1966) had been first seen in Hα line-center images as "winking" filaments that momentarily flickered out and back into view, always within minutes of an exceptionally bright flare in a neighboring region (Dodson 1949; Bruzek 1951; see references in Smith & Harvey 1971). The measured speed

[1] NSO Emeritus Astronomer.
[2] Operated by the Association of Universities Research in Astronomy (AURA), Inc., for the National Science Foundation.

TABLE 1
TIME SEQUENCE OF ACTIVITY IN THE 2002 DECEMBER 19 SOLAR ERUPTION

Time	Event ($t = 0$ at 21:35 UT)
−29 minutes (21:06 UT)	Onset of weak precursor event in soft X-rays and in Hα (see PFB in Fig. 3)
−19 to −16 minutes (21:16–21:22 UT)	Tiny rapid-rise preflare brightenings north of NOAA AR 228 (see points 1, 2, and 3 in Fig. 3)
−10 minutes (21:25 UT)	Activation of filament between NOAA ARs 224 and 226
−8 minutes	Southern portion of the TL has disappeared by this time
0 minutes (21:38 UT)	Main flare (2N/M2.7) onset (=20% of maximum brightening above background) in NOAA ARs 223 and 225; disturbance of central (transequatorial) Hα filament; inferred onset of CME rapid acceleration phase based on fast rise in soft X-ray curve (backward extrapolation using LASCO images leads to a CME onset time at −3 minutes); onset of sympathetic flare 1
+3 minutes (21:38 UT)	SCB A originates south of the NOAA AR 223/225/229 complex
+4 minutes (21:39 UT)	Onset of metric type II/IV radio bursts
+6 minutes (21:41 UT)	SCB B originates slightly to the west of SCB A
+6.5 minutes (21:41.5 UT)	SCB C follows in the path of A
+11 minutes (21:46 UT)	Onset of sympathetic flare 2
+14 minutes (21:49 UT)	Dimming region apparent in the first available 284 Å EIT image at the former location of the transequatorial loops (dimming may have already happened prior to this time); faint EIT wave
+18 minutes (21:53 UT)	Peak of M2.7 soft X-ray flare
+19 minutes (21:54 UT)	Reactivation of central filament
+22 minutes (21:57 UT)	SCB D originates slightly to the east of the central filament
+31 minutes (22:06 UT)	CME observed by LASCO in northwest quadrant, leading edge height of 4.2 $R_\odot$

of the visible chromospheric waves were initially found to be in the range 500–2000 km s^{-1}, and the propagating front was thought to be confined within a $\sim 90^\circ$ sector angle (Moreton 1960; Athay & Moreton 1961).

Smith & Harvey (1971) later identified two additional manifestations of the flare-wave phenomenon that are only seen in the core of the Hα line. These are (1) a hazy bright front emanating from the flare (see Glackin & Martin 1980) and (2) small fixed chromospheric structures that suddenly and successively brighten with distance from the flare. The mean speed of the waves inferred from oscillating filaments was 880 km s^{-1}, while the mean speed from measured wave fronts in the chromosphere was 600 km s^{-1} (Smith & Harvey 1971). Wider cone angles up to nearly 180° were observed or in some cases inferred. Although all four wave effects in Hα (bright/dark waves in the Hα line wings, winking filaments, diffuse fronts in the Hα line-center images, and sequential brightenings) have occasionally been observed within the same flare, more commonly only one or two effects are observed, suggesting different thresholds of detectability and possibly different physical mechanisms for each effect (Smith & Harvey 1971).

Two cases of "remote flare brightenings" without other reported flare-wave effects were studied by Tang & Moore (1982) and interpreted as the propagation of electrons along magnetic field lines connecting the flaring region with the chromospheric network on the quiet solar background. Supporting evidence for this was found in reverse-slope type III bursts and soft X-ray images.

Coronal (EIT) waves, observed with *SOHO* EIT, also appear as a bright front moving away from flares (Thompson et al. 1998, 1999, 2000b; B. J. Thompson et al. 2005, in preparation; Wills-Davey & Thompson 1999). Unlike Hα wave effects, however, coronal waves have been observed to completely surround the flare site, although a majority of the EIT waves have a more restricted span. EIT waves have measured front velocities ranging from $\sim$200 to 600 km s^{-1}; low image cadence may preclude measurements of higher speeds early in the events. The EIT waves at 195 Å are visible as sharp wave fronts early but become diffuse structures when observed far from the flare site. Chromospheric waves in Hα (also called Moreton waves) have been observed concurrently with EIT waves, but to date, direct comparisons of chromospheric and coronal waves have yielded conflicting results, with some authors favoring separate origins for the two phenomena (Eto et al. 2002; Chen et al. 2002) and others arguing for a unified picture (Warmuth et al. 2004a, 2004b; Cliver et al. 2004).

In this study, we describe a type of large-scale propagating disturbance that appears to be distinct from classic Moreton or EIT waves. We analyze ISOON Hα full-disk images and *SOHO* EIT/Michelson Doppler Imager (MDI) observations for a large-scale event on 2002 December 19 involving a halo CME that was associated with an erupting transequatorial loop (TL; see Delannée & Aulanier [1999], Khan & Hudson [2000], and Glover et al. [2003] for previously reported examples of such eruptions). The new aspect of the 2002 December 19 event revealed by high-cadence, high spatial resolution, ISOON Hα data is a series of sequential chromospheric brightenings (SCBs) that originate near the flare site and propagate across the solar equator along the path of the erupting TLs.

2. DATA SOURCES

2.1. *Chromospheric and Photospheric Observations*

Full-disk images of the Sun in Hα (line core, $\pm$0.4 Å) on 2002 December 19 were acquired using the ISOON telescope (Neidig et al. 1998). The images have a cadence of 1 minute and a sampling of 1.″1 pixel^{-1}. Photospheric magnetograms obtained by the *SOHO* MDI ($\sim$2″ pixel^{-1}; Scherrer et al. 1995) were also used in this study.

2.2. *Coronal Observations*

Coronal observations for this event were available from the *SOHO* EIT (Delaboudiniere et al. 1995) and the *SOHO* Large Angle Spectrometric Coronagraph (LASCO; Brueckner et al. 1995). The EIT images were obtained at 171, 195, and 284 Å. The average cadence of the 195 Å images was one image every 12 minutes, while 171 and 284 Å images were obtained once

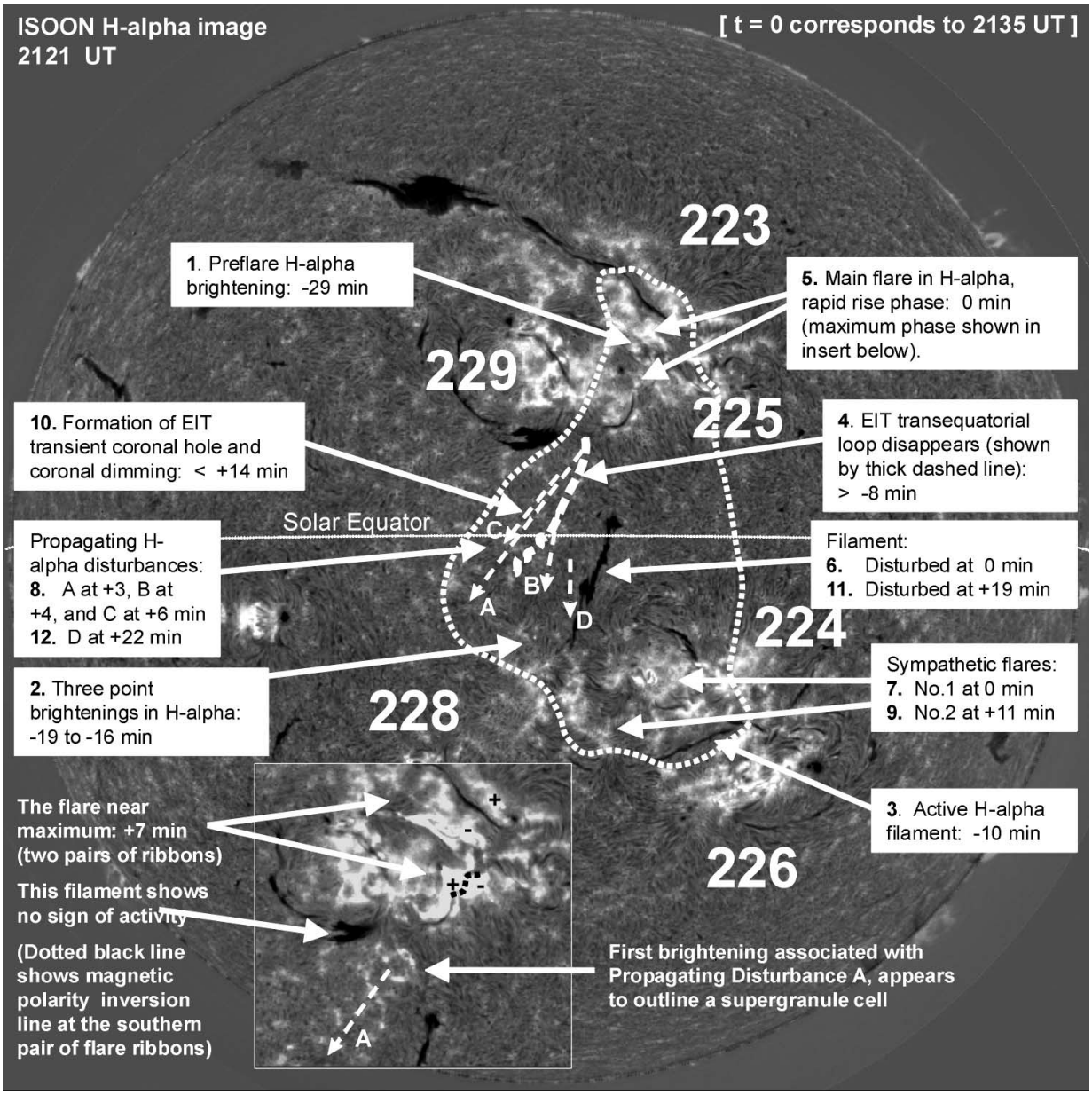

FIG. 1.—Full-disk ISOON Hα image on 2002 December 19. Sequence of activity observed in ISOON and EIT imaging data, shown in chronological order by number. All times refer to time of onset and are shown relative to 21:35 UT, which corresponds to the rapid rise phase of the main flare in Hα. The dotted white line shows the assumed boundary of the eruptive event based on the location of the main flare, the inferred propagating disturbances from the SCBs brightenings and sympathetic flares, filament activity, transient coronal hole formation, and point brightenings. Dashed arrows A, B, C, and D mark the paths of the SCBs. The inset shows the northern part of the activity. The magnetic neutral lines and polarities are marked in black.

every 6 hr. The LASCO images span a field of view of 2–30 $R_\odot$. The LASCO images have a cadence of ~30 minutes in the inner field of view (2–6 $R_\odot$) and ~60 minutes in the outer field of view (6–30 $R_\odot$).

3. THE SOLAR ERUPTION AT ~21:35 UT ON 2002 DECEMBER 19

3.1. *Sequence of Events*

The sequence of events in this eruption is summarized in Table 1. Included are preflare activity, main flare onset, CME launch, sympathetic flaring, and formation of the dimming region near the pre-eruption site of the TLs. The ISOON full-disk Hα image in Figure 1 and the EIT 284 Å images in Figure 2 give the locations of the various features/activities listed in Table 1. Note that the southern portion of the TLs shown in Figure 2*a* (EIT 284 Å images) appears to have disappeared prior to the onset of the main flare. A movie of the EIT 195 Å images show structural rearrangement of the entire TL system at the time of the flare. This may correspond to the CME launch *initiation* phase as described by Zhang et al. (2001). The dotted line in Figure 1 encompasses the various manifestations of the eruption and includes parts of at least four active regions (NOAA ARs 223, 225, 226, and 228).

3.2. *Sequential Chromospheric Brightenings*

Four series of sequential SCBs (identified from tracing individual images), designated series A, B, C, and D (arrows in Fig. 1 and letter prefixes in Fig. 3) progressively appear

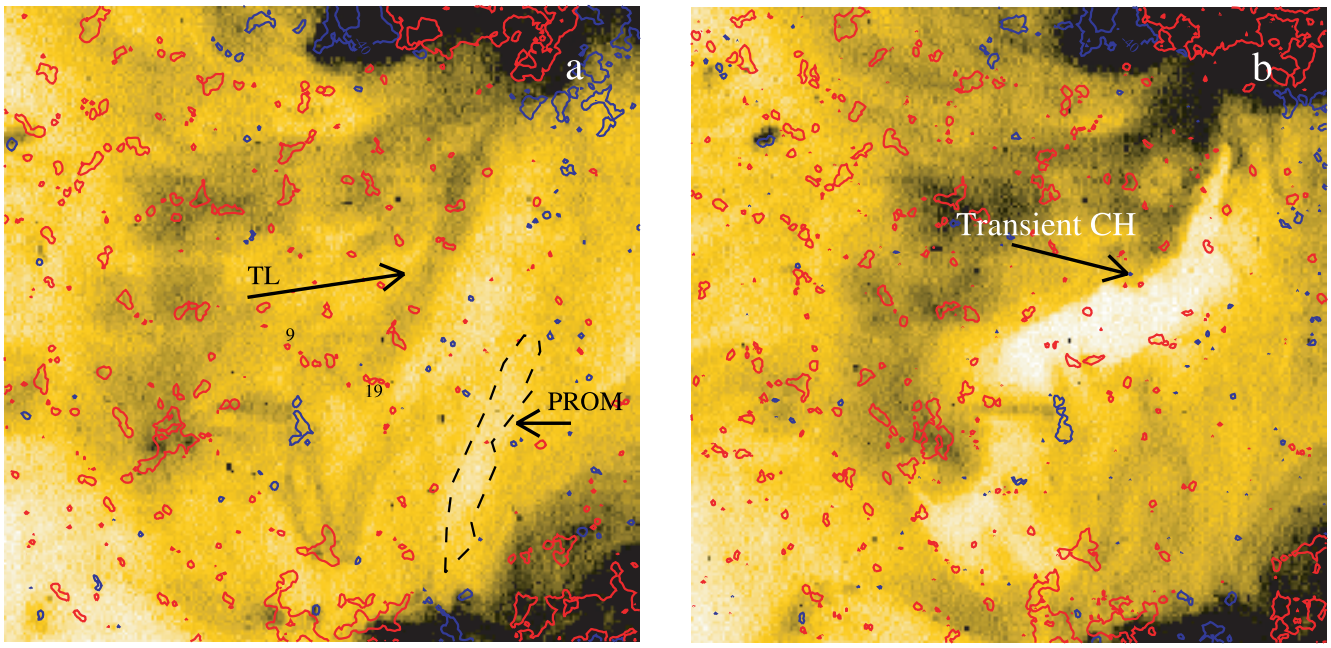

FIG. 2.—*SOHO* EIT images at 284 Å (*a*) before December 19 at 19:06 UT and (*b*) after December 20 at 01:06 UT, the eruption. MDI magnetic field contours of positive (*red*) and negative (*blue*) polarity are superposed. For reference, brightened points numbered 9 and 19 corresponding to points A9 and B19 in Fig. 3 are marked. Note the positions of the TL, filament (PROM), and transient coronal hole (CH).

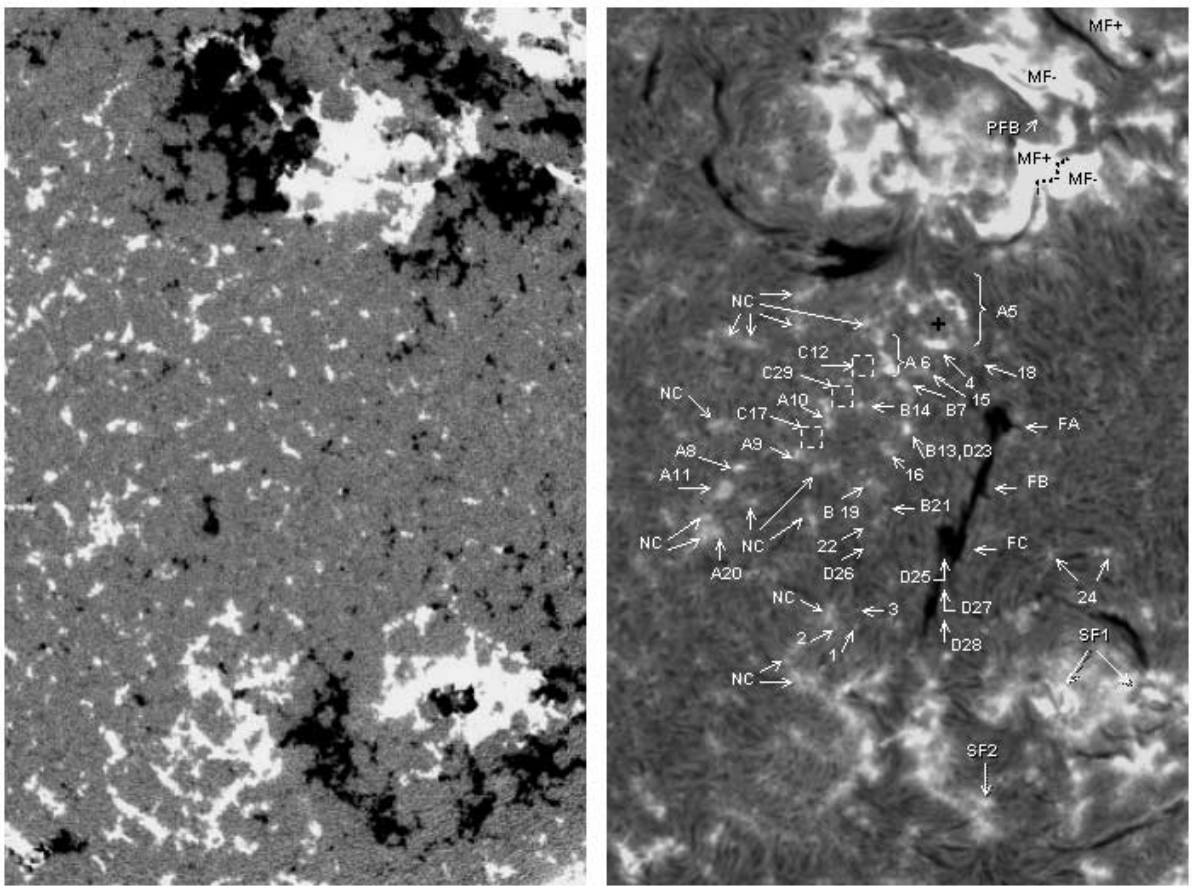

FIG. 3.—*Left*: MDI magnetogram, 20:51 UT, registered to the Hα image in the right panel. *Right*: Hα image showing chromospheric features that either brightened or moved during the eruptive event and its accompanying SCBs. MF: Main flare ribbon (with underlying photospheric magnetic field polarity indicated); dotted black line shows polarity inversion line. PFB: Preflare brightening. SF: Sympathetic flare. FA, FB, FC: Sections of filament that moved or changed during the event. The chromospheric network points that brightened and thus defined the SCBs are labeled by numbers prefixed by A, B, C, or D according to membership in their respective SCBs. These numbers are not assigned in chronological order of their appearance. D25, D27, and D28 refer to parts of the filament that moved in response to SCB D. Features without a letter suffix refer to network points that were observed to brighten but were not identified with an SCB because of their timing or location. Letters NC designate network points located in or near an SCB's path but that did not brighten. Points 1, 2, and 3 are precursor brightenings that appeared prior to the main flare.

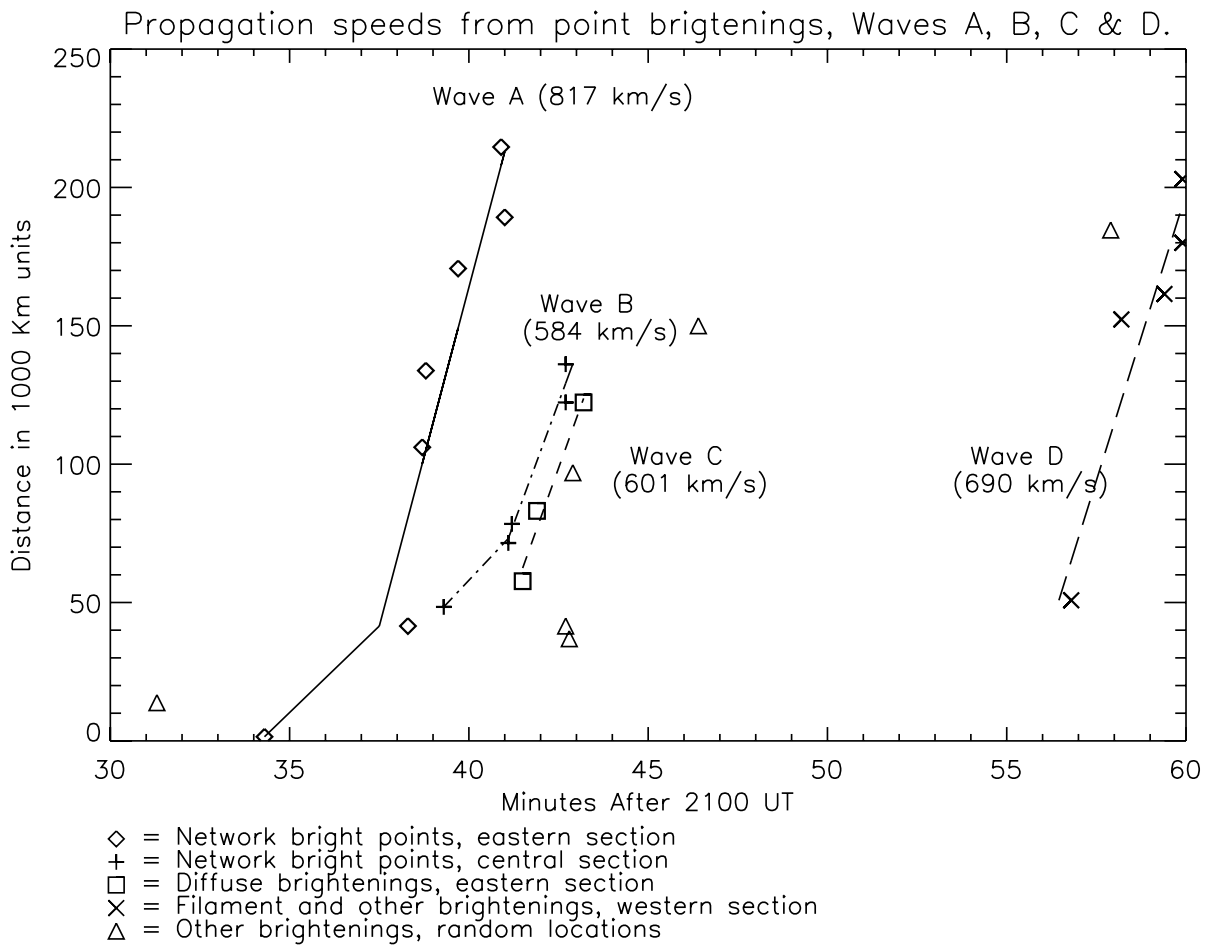

FIG. 4.—Time-distance plot showing the propagating speeds (the loci) of the chromospheric disturbances. Distances are measured from the plus sign at the center of the supergranule cell labeled A5 in Fig. 3.

southward of the active region in the northern hemisphere. The first, series A, begins at about 21:38 UT and the last, series D, begins at 21:57 UT. These four, suddenly appearing series of SCBs are separable on the basis of morphology, location, and time. In order to study the properties of these SCBs, we identified all features that either brightened, moved, or changed suddenly. These points are labeled in the Hα image in Figure 3*b*. Note that the image shown here is a single snapshot in time, so numerous features may not have been captured during their brightening, although their locations have been indicated. The timing was established by photometry of numerous features labeled by numbers and letters in Figure 3*b*.

We note the following changes for the SCB series A, B, C, and D, with reference also to features in Figure 3*b*.

1. Series A, B, and C occur in rapid succession and are overlapping in time (start times 21:38, 21:41, and 21:41.5 UT, respectively). Series B begins while series A is still in progress, but B is located to the west of A, and it illuminates different network points. Series C is nearly simultaneous with B but follows in the path of A. Series D begins much later, at about 21:57 UT.

2. SCBs A and B are brightenings of existing chromospheric network points. Rather than consisting of discrete points that brighten in sequence, series C appears as a diffuse brightening visible between the network points. Series D is also apparent in a sequential network brightening but also includes filament activation.

3. All of the SCBs, when traced back, appear to originate from the vicinity of a supergranule that shows an initial brightening at 21:34 UT (see the plus sign in Fig. 3*b* at feature A5).

4. Series D, in addition to including bright points, appears to be associated with the destabilization of the southern part of filament at FC. At a location southward of FB the filament partially erupts, and segment FC completely disappears. Segment FA remains after the event.

5. There is no discernible signature of these SCBs in the off-band Hα ($\pm$0.4 Å) images, obtained at the same cadence of 1 minute. Hence, there is no evidence of association with a classic Moreton-type chromospheric flare wave.

In Figure 4 we track the loci of the SCBs in a time-distance plot. The apparent "speeds" (in parentheses) correspond to the slopes of the least-squares fits to the steep portions of the curves. Different symbols are used to identify features that are perceived as distinctly different types of changes. While visual impressions may be subjective and even deceptive, the four different SCBs shown here are spatially, temporally, and morphologically separable in an objective sense, as described above. From the fits we see that SCBs A, B, C and D propagate at speeds of about 800, 600, 600, and 700 km s^{-1}, respectively. Note that speed in this limited context does not refer to actual waves but to loci of the brightenings.

By comparing Figure 3*b* with a corresponding MDI magnetogram (Fig. 3*a*) we find that all of the points that define the SCBs are of positive polarity (*white*). This magnetic monopolarity

association is very strong. Although not *all* of the white-poled points brighten, *none* of the black-poled points brighten. It is important to also note that white (positive) polarity seems to dominate in the region covered by the SCBs. If there is an exception to the monopolarity of brightened points, it involves the western component of the pair labeled 24, which is outside the area covered by the SCBs. This feature may actually be one of the footpoints of a bipolar mini flare.

3.3. *SOHO EIT and LASCO Observations of the Eruption*

A *SOHO* EIT 284 Å image at 19:06 UT shows TLs that join NOAA ARs 225 and 228. It appears that these TLs erupted to form a CME, first observed in the field of view of the LASCO C2 coronagraph at 22:06 UT at a height of 4.2 $R_\odot$. The 360° halo CME was most prominent in the northwest quadrant, and a speed of 1092 km s^{-1} was measured at a position angle of 300° (CME online catalog). The 284 Å image in Figure 2*b*, taken on December 20 at 01:06 UT, shows a transient coronal hole in the same location as the TLs on the previous day.

A movie sequence (12 minute cadence) of EIT images at 195 Å, between 21:27 and 22:24 UT, shows a flare brightening in the northern active regions. A movie sequence of running-difference EIT images indicates a faint radially propagating EIT wave, moving outward from the main flaring region and extending over ~200° from north of AR 225 in a clockwise direction to AR 228.

4. EXAMPLES OF SIMILAR PROPAGATING DISTURBANCES OBSERVED BY ISOON

We briefly mention three other similar events that we have studied, although they are not as complex as the 2002 December 19 event. None of them involved TLs.

1. On 2002 December 13, a C6 two-ribbon flare occurred with explosive ribbon expansion. An SCB with speed 60–70 km s^{-1} appears to be timed well for association with a flare brightening in a distant active region, and a large filament between the two active regions winks and oscillates in response.
2. On 2003 January 24, a C1 flare is accompanied by a multiribbon explosive event with violent filament eruption and two SCBs—one moving approximately parallel with the filament eruption and the other emanating at right angles to the filament motion. The speeds of the disturbances are difficult to measure but are of order 100 km s^{-1}. A flare is triggered in an active region in the direction of the ejected filament, nearly simultaneous with the initial flare and eruption.
3. On 2003 February 6, a small flare occurred without detectable *GOES* soft X-ray emission, but with a filament eruption and an SCB running in the same direction as the ejected filament, at a speed of 80 km s^{-1}.

These three similar eruptive events, while less impressive than the event on 2002 December 19, show most of the same phenomena, including distant sympathetic flares and SCBs. The SCB in the 2003 January 24 event did not strictly follow the monopolarity association.

Two of these events include filament eruptions near the main flare. We conclude that the observations of these four events are consistent with large-scale coronal eruptive activity that triggers nearly simultaneous surface activity of various forms separated by distances on the same scale as the coronal structures themselves.

5. DISCUSSION

In the 2002 December 19 event, a 2N/M2 multiribbon flare is one component of a collection of solar surface phenomena associated with a large coronal eruption. Our data are consistent with large-scale coronal eruptive activity that nearly simultaneously triggers several forms of widely separated surface phenomena encompassing several active regions as well as the area between them. The uniqueness of the data is demonstrated in the clarity and traceability of chromospheric phenomena associated with the event. The coronal manifestations include an opening/restructuring of magnetic fields, a halo CME, an EIT wave, and a coronal dimming. In the chromosphere, ISOON Hα images show distant flare precursor brightenings and sympathetic flaring. Originating near the main flare is a series of rapidly propagating (600–800 km s^{-1}), narrowly channeled SCBs that lie beneath the erupted TL. The partial eruption of the Hα filament that occurs in conjunction with the last SCB (D in Fig. 1) at about 21:54 UT could be either unrelated to or a secondary consequence of the CME. We infer that the rapid acceleration of the CME at ~21:35 UT occurs about 20 minutes prior to the partial filament eruption. This onset time is also coincident with the rapid rise phase of the soft X-ray event, as has been noted in a number of cases by Zhang et al. (2001).

The large-scale connectivity in the corona and in the lower atmosphere (chromosphere) has been considered in explaining sympathetic flares (e.g., Smith & Harvey 1971) or flare-associated chromospheric brightenings (Rust & Webb 1977). The use of the term "sympathetic" historically alludes more to the idea of a "synchronizing agent" (Fritzova-Svestkova et al. 1976) that could be responsible for the nearly simultaneous triggering of widely spaced chromospheric activity. We believe that the synchronizing agent in this case is the eruption of the overarching coronal structure that includes the CME launched at about the time of the main flare, or even before, when the TL disappears. The various precursor events (Fig. 1) that were observed at −29, −19, and −10 minutes before the main flare fall within a time frame consistent with the initiation phase of CMEs in general (Zhang et al. 2001). These unique data sets allow us to track a continuous stream of connected activity (flare, disappearing TLs, sequential brightenings, coronal dimming, halo CME), which strongly implies a large-scale connectivity beyond a simple coincidence of occurrences.

Sequential brightenings similar to those described herein were reported previously by Smith & Harvey (1971). The propagation speeds derived by Smith & Harvey for their events are consistent with ours. In contrast, some of the events observed by Smith & Harvey showed both continuous fronts (classical flare waves or Moreton waves) and sequential brightening of chromospheric points. In the event presented here (like those of Tang & Moore 1982) we see only the sequence of bright points, in the verified absence of a flare wave in the wings of the Hα line.

The eruption of TLs 8 minutes prior to the flare and the first noticed coronal dimming about +14 minutes after the flare also pose intricate issues in understanding the SCBs in conjunction with CMEs. For example, Gopalswamy et al. (1999) describe prolonged dimming preceding a TL eruption, which differs from the phenomena described here. Khan & Hudson (2000) suggest that TL eruptions are the result of shock waves originating from one of the associated active regions. In the observations of three events reported by them, the disappearance of loops last seen in *Yohkoh* soft X-ray telescope partial-frame images occurs within 0–3 minutes of the observation of a metric type II burst. The absence of high-cadence data for the coronal observations reported here stifles such a comparison. Suffice it to say that the TLs appear to have erupted before the onset of the flare.

Three possibilities can be hypothesized to explain the propagating sequential chromospheric brightenings: (1) A propagating

coronal shock might accelerate electrons on coronal field lines that are connected to chromospheric footpoints, (2) particles energized by the solar flare might follow specific field lines from the active region to the connecting network outside of the active region as described by Tang & Moore (1982), or (3) there may be a sequential tearing away of coronal field lines (by means of magnetic reconnection) during a CME. While we cannot completely rule out explanations 1 or 2, our data most strongly support explanation 3.

The latter interpretation is favored by the finding of Smith & Harvey (1971), that the events that were visible only as sequentially brightened points were the ones that were most directional; i.e., the arc of propagation was narrower than the waves that were seen as continuous fronts. A series of erupting coronal loops might restrict the affected field lines to a relatively narrow channel. In fact, in this case the SCBs are cospatial in the line of sight with the TL system that disappeared prior to the appearance of the SCBs. As the eruption proceeded to higher and higher loops, the connecting points of these loops in the lower atmosphere map farther from the active region with the primary flare. The fact that all of the brightened chromospheric points were of the same positive magnetic polarity is consistent with interpretations 2 and 3, but not interpretration 1. Shock fronts do not have a preference for the nature of the underlying magnetic polarity, and as a result one would, in some cases, expect brightening in both polarities. The replacement of the TLs by a dimming region (Fig. 2) favors explanation 3 over 2, because explanation 2 suggests a more static field geometry. (Recently, Gilbert & Holtzer [2004] have reported multiple large-scale waves seen from measurements in the He I 10830 Å line.)

The chromospheric events reported here differ from the counter parts of chromospheric flare waves and EIT coronal waves in the following aspects: (1) There is more than one SCB—a succession of SCBs—that are separated in time, and whose speeds are different, (2) the SCBs are the preferential brightening of network points belonging to one polarity, (3) the cluster of SCBs are confined to a small cone, subtending no more than 30°, and (4) the speeds for the SCBs described by the three additional events in § 4 are only 100 km s^{-1} or less, which is much slower than the speeds of coronal shock waves that produce classic Moreton waves and EIT waves. In addition, the directions of inferred motion of the coronal disturbances are nearly parallel with each other and follow the disappearance of erupting TLs. Although our data show only a faint EIT wave, it spreads in an expanding arc that is much wider than the narrow angle of the cluster of sequential chromospheric brightenings beneath the TLs. The He I 10830 Å observations for this event indicate a single wave propagating to the south of AR 229 and deflecting slightly to the west, i.e., in the general region occupied by the four SCBs we have identified (H. Gilbert 2005, private communication).

We propose the following phenomenological model as an explanation for the observed phenomena. An instability of the magnetic topology begins in the northern hemisphere about the complex of NOAA ARs 223, 225, and 229 before the main flare occurs. The eruption originates in the northern hemisphere. As the CME moves radially outward, it sequentially tears away multiple sets of field lines (by magnetic reconnection). Consequently, energetic electrons accelerated toward the chromosphere impact at the network points, resulting in the sequential brightenings. We suggest that the multiplicity of the SCBs reflects various strands of the transequatorial loop system that extends from AR 225 to AR 228. We envision a picture, supported by the magnetogram in Figure 3*a* and the monopolarity rule, in which each strand of the TL system consists of multiple nested loops with one set of footpoints located in AR 225 (to the north of the plus sign in Fig. 3*b*) and the other set extending progressively closer, loop by loop, to AR 228. The picture that we have in mind is one in which an eruption (CME), typically associated close in time with a flare (following Zhang et al. 2001) opens up field lines, creating a transient coronal hole or dimming (Thompson et al. 2000a).

Several models describe CME/flare eruptions as being due to an instability of interconnecting loops (e.g., Bagala et al. 2000; Wang et al. 2002). Delannée & Aulanier (1999) developed a CME model consisting of TLs and demonstrated that a bright disturbance can form as the result of the rapid opening of field lines during the eruption. The challenges of applying such models would be in the detailed modeling of the magnetic connectivity to individual polarities as seen by MDI high-resolution images, the tearing away of field lines, and the corresponding brightening of the Hα network.

ISOON is operated by the Air Force Research Laboratory, Space Vehicles Directorate, at NSO, Sunspot, NM. *SOHO* is a project of international cooperation between ESA and NASA. The LASCO CME catalog is generated and maintained by NASA and The Catholic University of America, in cooperation with the Naval Research Laboratory. A. A. P. acknowledges support from NASA grant NAG5-10852. The contributions of S. F. M. were supported by NSF grant ATM 02-09395.

REFERENCES

Athay, R. G., & Moreton, G. E. 1961, ApJ, 133, 935
Bagala, L. G., Mandrini, C. H., Rovira, M. G., & Demoulin, P. 2000, A&A, 363, 779
Brueckner, G. E., et al. 1995, Sol. Phys., 162, 357
Bruzek, A. 1951, Z. Astrophys., 28, 277
Chen, P. F., Wu, S. T., Shibata, K., & Fang, C. 2002, ApJ, 572, L99
Cliver, E. W., Nitta, N. V., Thompson, B. J., & Zhang, J. 2004, Sol. Phys., 225, 105
Delaboudiniere, J.-P., et al. 1995, Sol. Phys., 162, 291
Delannée, C., & Aulanier, G. 1999, Sol. Phys., 190, 107
Dodson, H. W. 1949, ApJ, 110, 382
Dodson, H. W., & Hedeman, E. R. 1964, in the Physics of Solar Flares, ed. W. N. Hess (NASA SP-50; Washington: NASA), 15
———. 1968, Sol. Phys., 4, 229
Eto, S., et al. 2002, PASJ, 54, 481
Fritzova-Svestkova, L., Chase, R. C., & Svestka, Z. 1976, Sol. Phys., 48, 275
Gilbert, H. R., & Holtzer, T. E. 2004, ApJ, 610, 572
Glackin, D., & Martin, S. F. 1980, Proc. SPIE, 264, 236
Glover, A., Harra, L. K., Matthews, S. A., & Foley, C. A. 2003, A&A, 400, 759
Gopalswamy, N., Kaiser, M. L., MacDowall, R. J., Reiner, M. J., Thompson, B. J., & St. Cyr, O. C. 1999, in AIP Conf. Ser. 471, Proc. Ninth Int. Solar Wind Conf., ed. S. R. Habbal et al. (New York: AIP), 641
Khan, J., & Hudson, H. 2000, Geophys. Rev. Lett., 27, 1083
Moreton, G. E. 1960, AJ, 65, 494
Neidig, D., et al. 1998, in ASP Conf. Ser. 140, Synoptic Solar Physics, ed. K. S. Balasubramaniam, Jack Harvey, & D. Rabin (San Francisco: ASP), 519
Ramsey, H. E., & Smith, S. F. 1966, AJ, 71, 197
Rust, D., & Webb, D. 1977, Sol. Phys., 54, 403
Scherrer, P. H., et al. 1995, Sol. Phys., 162, 129
Smith, S. F., Harvey, K. L. 1971, in Physics of the Solar Corona, ed. C. M. Marcis (Dordrecht: Reidel), 156
Tang, F., & Moore, R. L. 1982, Sol. Phys., 77, 263
Thompson, B. J., Cliver, E. W., Nitta, N., Delannée, C., & Delaboudinière, J.-P. 2000a, Geophys. Rev. Lett., 27, 1431
Thompson, B. J., Plunkett, S. P., Gurman, J. B., Newmark, J. S., St. Cyr, O. C., & Michels, D. J. 1998, Geophys. Res. Lett., 25, 2465

Thompson, B. J., Reynolds, B., Aurass, H., Gopalswamy, N., Gurman, J. B., Hudson, H. S., Martin, S. F., & St. Cyr, O. C. 2000b, Sol. Phys., 193, 161
Thompson, B. J., et al. 1999, ApJ, 517, L151
Wang, H., Gallagher, P., Yurchyshyn, V. Yango, G., & Goode, P. R. 2002, ApJ, 569, 1026
Warmuth, A., Vršnak, B., Magdalenić, J., Hanslmeier, A., & Otruba, W. 2004a, A&A, 418, 1101
———. 2004b, A&A, 418, 1117
Wills-Davey, M. J., & Thompson, B. J. 1999, Sol. Phys., 190, 467
Zhang, J., Dere, K. P., Howard, R. A., Kundu, M. R., & White, S. M. 2001, ApJ, 559, 452